Langmuir Probe Investigations of Different Magnetic Filter Field Configurations at BATMAN Upgrade

L. Schiesko, C .Wimmer and U. Fantz

Max-Planck-Institut für Plasmaphysik, Boltzmannstrae 2, 85740 Garching, Germany

loic.schiesko@ipp.mpg.de

Abstract. Langmuir probe measurements were performed at the newly commissioned BATMAN Upgrade test bed to determine the plasma parameters in front of the plasma grid (PG). At BATMAN Upgrade, the magnetic filter field can either be generated by permanent magnets or by a current of several kilo-amperes flowing through the plasma grid. Although achieving similar strength in front of the plasma grid, the two magnetic field configurations show very different topology. The topology strongly affects the transport of the charged particles from the driver towards the plasma grid and Langmuir probes show different positive ion density and asymmetry in front of the PG.

INTRODUCTION

For the international fusion experiment ITER, large and powerful negative hydrogen ion sources are mandatory for the neutral beam injection (NBI). For heating and current drive (HNB) two beam lines are designed to inject 33 MW total power at a beam energy of 870 keV H^0 or 1 MeV D^0 for up to 3600 s [1]. Negative ion currents of 66 A in hydrogen and 57 A in deuterium must be extracted from the ion source at a pressure of 0.3 Pa in order to fulfil these requirements.

Since 2007, the Max-Planck-Institut für Plasmaphysik (IPP) RF driven negative ion source prototype [2, 3, 4] is the reference design to equip the ITER neutral beam injectors [5]. The test facility which holds the prototype source, BATMAN, was dedicated to the understanding of physical processes due its large variety of diagnostics and its high flexibility as well as to the optimization and development of the ion source. The BATMAN test bed was upgraded during 2017 and is now commissioned. While the ion source remain unchanged (prototype ion source), major hardware upgrades were undertaken to improve crucial aspects of the test bed and in particular the beam physics with the design of a new grid system with ITER-like aperture geometry and size, an increase of the total high voltage. Additionally, the installation of an ITER-like magnetic field configuration (MF) generated by a current vertically driven into the first grid of the extraction system, the plasma grid (PG) was made. Furthermore, improvements diagnostics were made, as for example an increased number of available line of sight both for beam and optical emission spectroscopy. As an another example, a tungsten wire calorimeter located near the grounded grid (GG) and monitored by a camera was installed as new beam diagnostic.

Alongside at IPP, the ELISE test facility [6, 7, 8] (1/2 area of the ITER ion source) is operated to demonstrate the scalability to larger areas of the small size prototype ion source. ELISE is an important intermediate step towards the realization of the ITER neutral beam injection system because the gained early operational experience gives valuable input for the design, commissioning and operating phase of the European Neutral Beam Test Facility (NBTF) PRIMA in Padova [9]. NBTF consists of the full ITER size 100 kV SPIDER facility [10] operational since 2017 and the 1 MV MITICA facility [11, 12] still under construction.

The work principle of H^- (D^-) ion sources is still based on the conversion of atomic neutrals and positive hydrogen ions (to a lower extent) into negative ions on all the source surfaces [13, 14]. However for the presented results, the source was completely free of Cs: no Cs was evaporated before or during the measurements.

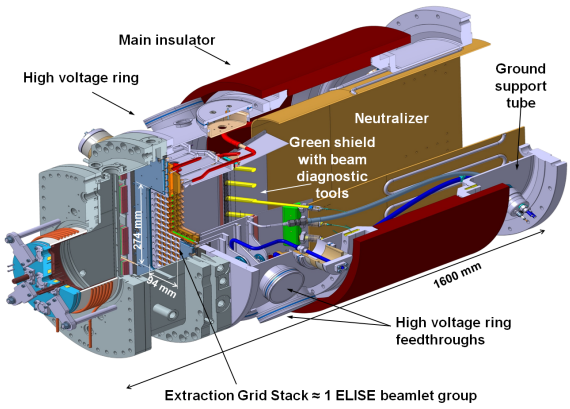

FIGURE 1. Schematic representation of BATMAN Upgrade.

The extraction was also not applied.

This paper reports first Langmuir probe measurements performed at BATMAN Upgrade in the PG vicinity with hydrogen gas. The results were obtained for different magnetic field configurations, pressures and power. The positive ion densities, electron temperature and plasma homogeneity were derived from I-V curves.

In section II are presented the experimental setup and the Langmuir probes, followed by a presentation and a discussion of the results in section III.

Experimental setup and diagnostics

In the following paragraphs only some upgrades and the Langmuir probe diagnostic will be detailed. A more complete description of the experimental setup and new diagnostics is left for a forthcoming publication.

Experimental setup

The experiments were performed on BATMAN Upgrade test bed schematically represented in fig. 1 and the source was completely free of Cs. BATMAN Upgrade is a pulsed test bed with 5 s extraction out of 10 s plasma pulse with a duty cycle of roughly 180 s. The hydrogen plasma is generated in the driver by a 1 MHz RF solid state generator with a maximum power of 150 kW. A Faraday shield is installed in the driver to protect the alumina cylinder from the plasma.

The driver plasma diffuses in the expansion region and reaches the extraction region where most of the extracted negative ions are generated. The driver and expansion region are separated by a magnetic field intended to cool down the electron temperature in order to reduce the destruction of negative ions by electron collision and to lower the amount of electrons inevitably co-extracted with the negative ions. The amount of co-extracted electrons has to be minimized to avoid damages in the extraction system. An electron temperature lower than 2 eV should be achieved as the main negative ion destruction mechanism -electron collisions- cross section strongly drops below this temperature. At BATMAN, the MF was only generated by permanent magnets either embedded in the diagnostic flange shown in fig. 2 or installed in a frame movable along the expansion region [15]. At BATMAN Upgrade, an additional MF configuration is available by driving vertically a current up to $I_{PG} = 3$ kA into the PG. The MF strength at the PG centre roughly scale as 1.5mT/kA. Fig. 2 presents the horizontal 2D maps for the different magnetic field configurations. The MF topology is very different when comparing permanent magnets and I_{PG} MF. Although comparable intensity is achieved in front of the PG centre as shown in fig. 3, the transport of both the electrons and positive ions from the driver towards the PG is affected by the topology as will be discussed below.

The PG is the first grid of the extraction system, now comprising four grids for a total high voltage (HV) of -50 kV i.e. roughly thirty percent more than former BATMAN hardware capabilities (see[17] for more details on the

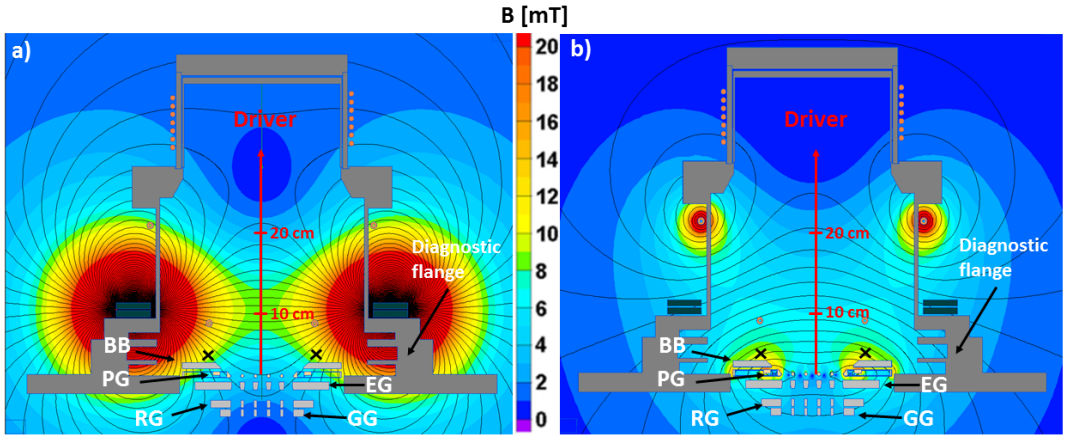

FIGURE 2. Horizontal 2D maps from two of the used magnetic field configurations: a) MR, 2x4, z = 9, b) I_{PG} = 3 kA. The crosses represents the approximative locations of the Langmuir probe tips.

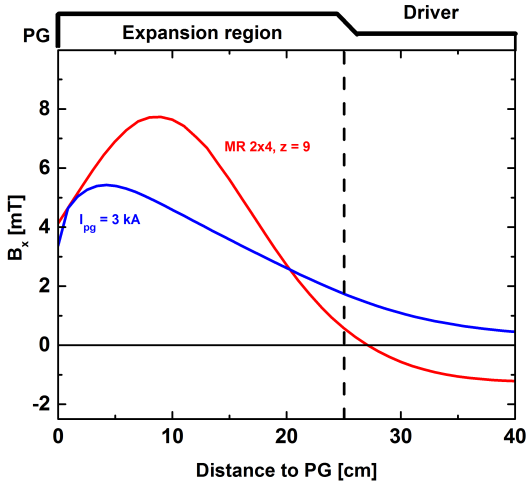

FIGURE 3. Horizontal magnetic field profiles for different configurations taken in the centre of the ion source i.e. along the vertical arrow in fig 2a and 2b.

new extraction system).

Most of the electrical and cooling systems were redesigned to improve the reliability. Additionally, a cryogenic pump will be soon installed to replace one of the two titanium sublimation pumps with the goal to improve the stability of the pressure during pulses. Furthermore, the electrical, cooling systems and the pumping system including the cryogenic pump are suited to cw plasma and beam operation planned in a near future.

Diagnostics

Source and beam diagnostics are described in [17] and will not be mentioned with the exception of Langmuir probes and analysis procedure.

Two symmetrically arranged non-RF compensated pin probes were used during this study to determine the plasma parameters in the PG vicinity. Their location, indicated in fig. 4, allows the determination of the local plasma parameters. The probe tip is situated at a distance of 0.75 cm from the bias plate. The tungsten probes tip radius and length are 150 μm and 1 cm respectively. The Langmuir probe acquisition system was previously described in detail

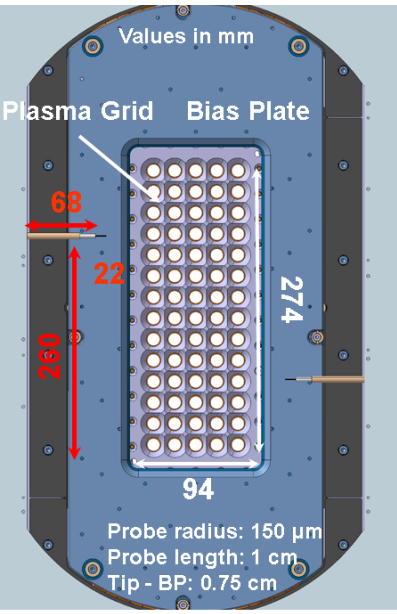

FIGURE 4. Location of the Langmuir probes. The upper probe is labelled top, while the lower probe is labelled bottom. All the units are in mm except when specified.

[18].

The presence of a magnetic field can be an issue in the evaluation of the electron density from the probe characteristic due to the electron following the magnetic field lines, which can lead near the permanent magnets to mirror effect. The effects of a magnetic field on the electron branch can lead to a reduction of the electron current to such an extent that the linear Maxwellian region is absent. At the location of the probes tips, the magnetic field strength is around 15 mT when considering the permanent magnets configuration. An estimation of the electron gyroradius for $T_e = 1$ eV yield 160 μm which is slightly larger than the probe radius. Because the magnetic tube surface area for a radius equal to the electron gyroradius does not significantly exceed the probe surface area, determining the electron density from the electron saturation current at the plasma potential would yield inaccurate results.

Additionally, because the probes are not RF compensated, the evaluation of the plasma potential from the 0 crossing point of the I-V curve second derivative would also yield inaccurate results. In order to overcome these issues it is possible to analyse the high energy part of the I-V electron branch, below the floating potential [19]. The clear advantage of using the high energy part of the electron branch is that the electrons are less affected by RF fluctuations and possess a larger Larmor radius.

For voltages lower than the floating potential, the probe current is made of positive ions and electrons. An accurate fit of the ion branch current has to be performed first in order to substract the ion current of the total I-V curve current to analyze the remainig high energy part of the electron branch [19].

The ion branch could be well fitted with the Langmuir's OML formula [20, 21] yielding the positive ion density. An effective mass of 1.8 a.m.u. was used to compute the positive ion density. It corresponds to an ion proportion of 40% H^+, 40% H_2^+ and 20% H_3^+, which was measured on a source functionally identical to the driver of the ion source used in this study [22]. The positive ion density is by far the most accurate plasma parameter because positive ions are not affected by RF and not magnetized in the present conditions. After substraction of the ion current of the total current I-V curve, the electron temperature and plasma potential could be derived from the fit of the remaining high energy electron part following the same procedure as described in [19].

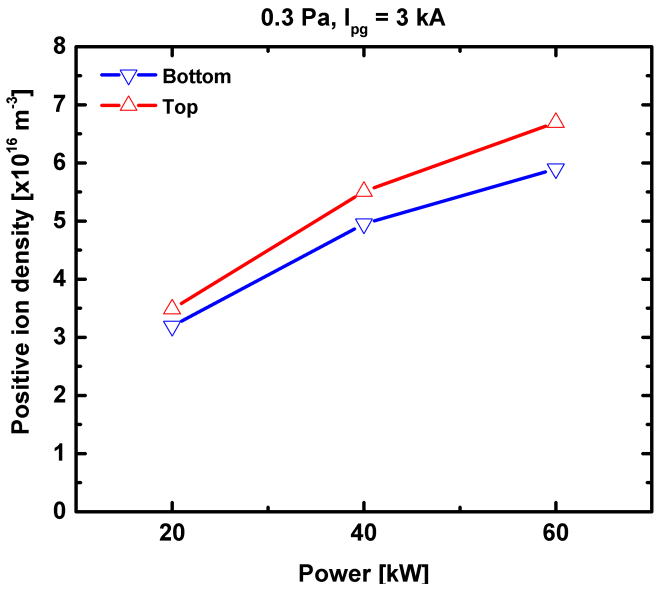

FIGURE 5. Variation of the positive ion density evaluated from the top and bottom I-V curves as a function of the injected RF power for 0.3 Pa pressure and I_{PG} = 3 kA.

Experimental results and discussion

The experiments were conducted in hydrogen at 40 kW of injected RF power, in a Cs-free source and without HV extraction.

Fig. 5 shows the variation of the positive ion density evaluated from the top and bottom probes characteristics at a pressure of 0.3 Pa and I_{PG} = 3 kA for different values of injected RF power. A quasi linear increase with the RF power of the positive ion density is observed. The electron temperature remained basically the same at around 2 eV (not shown here). Similar trends with the positive ion density were also observed with the other MF configurations.

Fig. 6 shows the variation of the electron temperature T_e for the top and bottom probes at 0.3 and 0.6 Pa for different magnetic field strength and configurations. No clear difference between T_e evaluated by the top and bottom probe can be seen. As expected, the largest T_e is observed without MF. Moreover, the change in the diffusion balance between 0.3 and 0.6 Pa is responsible for the smaller T_e. For the two pressures, $T_e < 2$ eV can be achieved and very close values for the electron temperature are measured with both I_{PG} and the permanent magnets configurations for comparable MF strength at the PG centre.

In [23], axial measurements of the plasma parameters were made by two vertically arranged Langmuir probes that could be moved from the driver exit to the PG vicinity. A comparison of the electron temperature measured in [23] for the same source and permanent magnets MF configuration as used in this study (0.6 Pa H_2, 40 kW RF power discharge with 2x4 z = 9 MF configuration) shows that around 1.2 eV is measured in this study while roughly 0.8 eV is shown in [23]. One could have expected a lower T_e for the present study as the probe was located near the PG while no measurement with a distance lower than 6 cm from the PG could be made in [23]. However as shown in fig. 3, the MF topology for the permanent magnets leads to a stronger MF strength in a larger part of the expansion region than with I_{PG} which may explain the lower Te values. Nevertheless, the values of the electron temperatures evaluated for the two studies agree within the error bars.

Recently, Lishev [24] investigated the influence of the MF topology (permanent magnets and I_{PG} configurations) on the discharge structure by simulating the variation of the plasma parameters with a 2D fluid model applied to the prototype ion source at 0.6 Pa H_2 and 40 kW of injected RF power. For the different MF configurations, the computed values of T_e in [24] are in fair agreement with the measurements presented here.

The variation of the positive ion density for the top and bottom probes at 0.3 and 0.6 Pa for different magnetic field strength and configurations is presented in fig. 7. The positive ion density measured for the I_{PG} are slightly

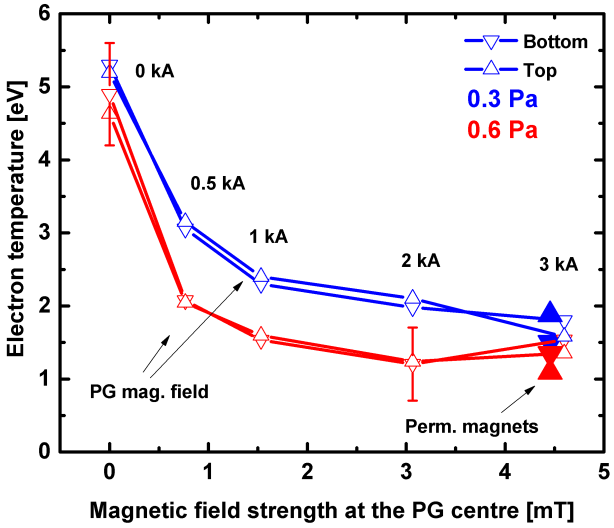

FIGURE 6. Variation of the electron temperature evaluated from Langmuir probes I-V curves as a function of the MF strength at the PG centre for two pressures. For the I_{PG} MF configuration, the corresponding current is indicated as label.

larger than with permanent magnets configuration. When comparing the MF 2D maps in fig. 2 one sees that for the permanent magnets, the strength of the MF lines intercepting the walls is much larger 10 cm before reaching the PG than with I_{PG}. As a consequence, the electrons are more magnetized in this region with the permanent magnets, and thus more losses on the walls could occur at this location, leading to a slightly lower density in front of the PG.
Moreover, the values presented here at 0.6 Pa for the permanent magnets are lower than the ones shown in [23] which is likely due to the fact that the previous measurements could not be done closer than 6 cm from the PG.
However, a good agreement is found between the positive ion density (the electron density is shown in Lishev's paper instead of the positive ion density) computed in [24] and the presented results with the I_{PG} at 0.6 Pa.
Figure 7 also show that an increase of I_{PG} has almost no influence on the measured positive ion density. The trend shown here at 0.6 Pa is in agreement with calculations made in [24] where no strong dependence from the positive ion density to the I_{PG} MF strength was found.

Another interesting feature is that in contrast to the permanent magnets configuration where a difference between the positive ion density evaluated from top and bottom probes is observed, almost no difference is seen with the I_{PG} configuration.

To better highlight this difference, fig. 8 shows the variation of the asymmetry factor defined as

$$\frac{n_i^{Top}}{n_i^{Bot}} \tag{1}$$

with n_i^{Top} and n_i^{Bot} being the top and bottom positive ion density respectively for different pressures and MF configurations.
It clearly appears from fig. 8 that the positive ion density in front of the PG is more symmetric in any case with the I_{PG} than with the permanent magnets configuration.
The asymmetry in the positive ion density is clearly due to the presence of the MF as experimentally shown in [23] when comparing measurements with and without MF, while 2D modelling highlighted the importance of ExB and diamagnetic drifts [25] on the transport of the particles towards the PG by showing they were responsible for density and temperature gradients in the expansion region and near the PG. As a consequence for the lowest values of I_{PG} one expects to observe a smaller asymmetry as it is the case in fig. 8. However it is surprising to see that for comparable MF strength in front of the PG, the permanent magnets show a much larger asymmetry than $I_{PG} = 3$ kA in fig. 8. This

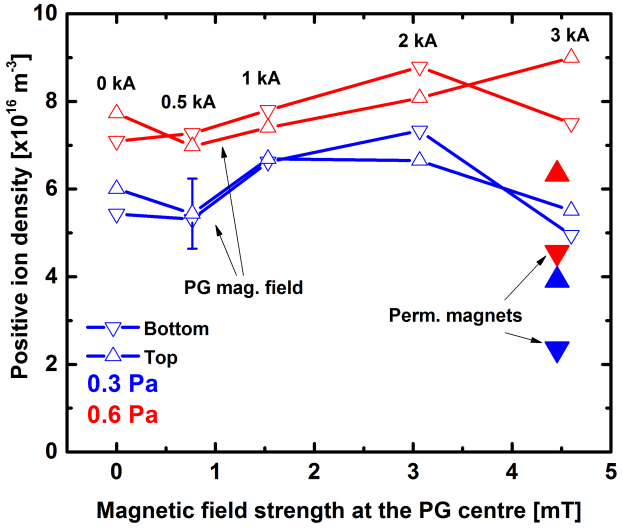

FIGURE 7. Variation of the positive ion density evaluated from Langmuir probes I-V curves as a function of the MF strength at the PG centre for two pressures. For the I_{PG} MF configuration, the corresponding current is indicated as label.

observation is probably due to the very different magnetic field topology between the I_{PG} and the permanent magnets as highlighted in fig. 2 but also to the lower maximum strength achieved by the I_{PG} in the expansion region. A larger magnetic field strength leads to stronger ExB and diamagnetic drift, and hence, the transport of the charged particles from the driver towards the PG is more affected.

The presented measurements clearly show that the plasma asymmetry in front of the PG can be strongly improved when using a MF whose topology is smoother than with permanent magnets.

The positive ion asymmetry in front of the PG as well as the MF topology are critical parameters that may affect both the Cs redistribution on the PG by the plasma and the beam homogeneity. An important aspect of the forthcoming BATMAN Upgrade campaign will be to determine the influence of the MF configuration on both the beam homogeneity and Cs redistribution in the PG vicinity by means of beam emission spectroscopy and the different calorimeters on one side, and the laser absorption on the other side.

Conclusion

BATMAN Upgrade is now commissioned. Many critical aspects of the test bed were upgraded. Among them, an increase of total available HV to 50 kV together with a new ITER-like grid system and the possibility to generate the MF by a current vertically flowing through the PG.
When comparing I_{PG} to permanent magnets, comparable magnetic field strength values can be achieved in front of the PG, however the topology of and maximum value of the field are very different. Langmuir probes measurements located in the PG vicinity showed that comparable electron temperature could be achieved. Furthermore, an improvement of the positive ion asymmetry when using the new MF configuration I_{PG} was observed. A modification of the transport of the electrons and positive ions from the driver towards the PG is induced by the smoother topology of the I_{PG} MF when compared to the permanent magnets. The trends of the presented results are supported by 2D fluid modelling.
Measurements of the changes induced by the MF on the beam and Cs redistribution will be performed in forthcoming campaign.

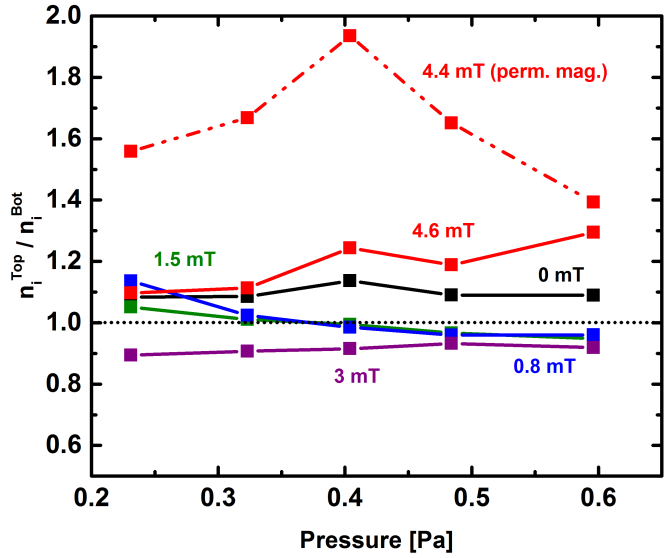

FIGURE 8. Variation of the positive ion asymmetry defined as n_i^{Top}/n_i^{Bot} as a function of the MF strength at the PG centre for different pressures. For the I_{PG} MF configuration, the corresponding current is indicated as label.

REFERENCES

[1] Schunke B., Bora D., Hemsworth R. and Tanga A., AIP Conf. Proc. 1097 (2009) 480.
[2] Speth E. et al., Nucl. Fus. 46 (2006) 220.
[3] Franzen P. et al., Nucl. Fus. 47 (2007) 264.
[4] Schiesko L. et al., Plas. Phys. & Cont. Fus. 53 (2011) 085029.
[5] Hemsworth R., Tanga A. and Antoni V., Rev. Sci. Inst. 79, (2008) 02C109.
[6] Fantz U. et al., Rev. Sci. Inst. 85 (2014) 02B305.
[7] Bonomo F. et al., Plas. Phys. & Cont. Fus. 56 (2014) 015006.
[8] Franzen P., Fantz U., Wünderlich D., Heinemann B., Riedl R., Kraus W., Fröschle M., Ruf B., Nocentini R. and the NNBI Team, Nucl. Fusion 55 (2015) 053005.
[9] Sonato P., Bonicelli T., Chakraborty A.K., Hemsworth R., Watanabe K., Day C., Franzen P. and Waldon C. 2010 The ITER neutral beam test facility in PaduaItaly: a joint international effort for the development of the ITER heating neutral beam injector prototype Proc. 23rd IAEA Fusion Energy Conf. (Daejeon, Korea, 2010)
[10] P. Sonato et al., Fusion Eng. Des. 84, (2009) 269.
[11] Chitarin G. et al., Rev. Sci. Instrum. 83 (2012) 02B107.
[12] Singh MJ. Boilson D., Hemsworth R. et al., IEEE Trans. on Plasma Science 44 (2016) 1496-1505.
[13] Belchenko Yu. I., Dimov G. I., and Dudnikov V. G., Nucl. Fus. 14 (1974) 113-114.
[14] Belchenko Yu. I., Dimov G. I., and Dudnikov V. G., Proc. Symp. Production and Neutralization of Negative Hydrogen Ions and Beams, Brookhaven, 1977 (BNL, Upton, NY, 1977).
[15] Franzen P., Schiesko L., Fröschle M., Wünderlich D., Fantz U. and the NNBI Team, Plasma Phys. Control. Fusion 53 (2011) 115006.
[16] Fantz U. et al., Rev. Sci. Instrum. 79 (2008) 02A511.
[17] Kraus W., Schiesko L., Fantz U. and Heinemann B., this conference.
[18] McNeely P., Dudin S. V., Christ-Koch S., Fantz U. and NNBI Team, Plasma Sources Sci. Technol. 18 (2009) 014011.
[19] Chen FF., Plasma Sources Sci. Technol. 21 (2012) 055013.
[20] Mott-Smith H. M. and Langmuir I., Phys. Rev. 28 (1928) 727.
[21] Chen FF., Plasma Sources Sci. Technol. 18 (2009) 035012.
[22] Rust N. et al 2002 Fusion Engineering and Controlled Fusion (Montreux, Switzerland, 1721 June 2002) published on CD-ROM.
[23] Schiesko L., McNeely P., Franzen P., Fantz U. and the NNBI Team, Plasma Phys. Control. Fusion 54 (2012) 105002.
[24] Lishev St., Schiesko L., Wünderlich D. and Fantz U. AIP Conference Proceedings 1869 (2017) 030042.
[25] Lishev St., Schiesko L., Wünderlich D. and Fantz U. AIP Conference Proceedings 1655 (2015) 040010.